



Effect of cold air plasma on the morphology and thermal stability of bleached hemp fibers

Efecto de plasma frío de aire sobre la morfología y estabilidad térmica de fibras de cáñamo blanqueadas

F.J. Alonso-Montemayor¹, C.M. López-Badillo¹, C.N. Aguilar¹, F. Ávalos-Belmontes¹, A.O. Castañeda-Facio¹, R. Reyna-Martínez¹, M.G. Neira-Velázquez², G. Soria-Argüello², D. Navarro-Rodríguez², M. Delgado-Aguilar³, R.I. Narro-Céspedes^{1*}

¹Universidad Autónoma de Coahuila (UAdeC). Facultad de Ciencias Químicas (FCQ). 25280, Saltillo, Coahuila, México.

²Centro de Investigación en Química Aplicada (CIQA). 25294, Saltillo, Coahuila, México.

³Grupo LEPAMAP, Departamento de Ingeniería Química, Universidad de Girona (UdG). 17003, Girona, Cataluña, España.

Received: March 28, 2020; Accepted: May 20, 2020

Abstract

The use of cold plasma surface modification techniques has lately gained increasing interest as a complementary option (non-pollutant and free of hazardous chemicals) to increase the thermal stability of bio-based fibers, and thus make them more suitable for polymer reinforcing applications. A considerable amount of studies has been performed to improve the thermal stability of “raw” lignocellulosic fibers by using cold plasma. Only few studies were done using “bleached” ones. Bleaching is mainly applied to increase the reinforcing capacity of fibers. Improving the thermal stability of bleached fibers is needed to reduce or avoid their degradation during the processing of bio-based composites. In this study, commercial bleached hemp (CBH) fibers were modified using low-pressure rotary air plasma (LPRP) and atmospheric-pressure air plasma jet (APPJ) devices to be further characterized by Fourier transform infrared spectroscopy–attenuated total reflectance mode (FTIR-ATR), X-ray diffraction (XRD), scanning electron microscopy (SEM), and thermogravimetric analysis (TGA). FTIR analysis evidenced the oxidation and crosslinking of cellulose chains. XRD analysis revealed a slight increase in interplanar distances of cellulose chains, that was attributed to the interchain insertion of functional groups. SEM images displayed much rougher surfaces for the treated CBH fibers than for the untreated one. TGA showed that LPRP (30 min treatment) and APPJ increased the thermal resistance of CBH fibers, which exhibited an initial degradation temperature 15 and 30 °C higher than that of the untreated fiber, respectively. For LPRP, a longer exposition time (180 min) provoked significant eroding without improving the thermal resistance. Finally, the cold plasma surface modification of bleached hemp fibers may well assist with the mechanical interlocking and thermal resistance (during processing) when applied in polymer reinforcing.

Keywords: Plasma jet, low-pressure plasma, hemp fiber, thermal stability, cellulose.

Resumen

El uso de técnicas de modificación de superficies por plasma frío ha venido ganando un interés creciente como una opción complementaria (no contaminante y libre de químicos peligrosos) para incrementar la estabilidad térmica de fibras bio-basadas, haciéndolas más aptas para reforzar polímeros. Una cantidad considerable de estudios han sido llevados a cabo para incrementar la estabilidad térmica de fibras lignocelulósicas “vírgenes” usando plasma frío. Pocos estudios fueron hechos con fibras “blanqueadas”. El blanqueamiento es principalmente aplicado para incrementar la capacidad reforzante de las fibras. Mejorar la estabilidad térmica de fibras blanqueadas es necesario para reducir o evitar la degradación de las fibras durante el procesamiento de compósitos bio-basados. En este estudio, fibras comerciales de cáñamo blanqueado (CBH) fueron modificadas usando dispositivos de plasma de aire de baja presión tipo rotatorio (LPRP) y plasma de aire a presión atmosférica tipo jet (APPJ) para ser posteriormente caracterizadas mediante FTIR-ATR, XRD, SEM y TGA. El análisis por FTIR evidenció la oxidación y entrecruzamiento de las cadenas de celulosa superficiales. El análisis por XRD reveló un incremento en la distancia interplanar de las cadenas de celulosa, lo cual fue atribuido a la inserción de grupos funcionales entre cadenas. El análisis por SEM mostró una superficie mucho más rugosa para CBH tratadas que para las no tratada. TGA mostró que los tratamientos por LPRP (30 min) y APPJ incrementaron la resistencia térmica de las fibras de CBH en 15 y 30 °C, respectivamente. Para LPRP, una exposición más extendida (180 min) provocó una erosión significativa sin mejorar la resistencia térmica. Finalmente, la modificación con plasma frío de la superficie de las fibras de cáñamo blanqueado puede ayudar al acoplamiento mecánico y resistencia térmica (durante el procesamiento), cuando sean aplicadas en el reforzamiento de polímeros.

Palabras clave: Plasma jet, plasma de baja presión, fibra de cáñamo, estabilidad térmica, celulosa.

* Corresponding author. E-mail: rinarro@uadec.edu.mx

<https://doi.org/10.24275/rmiq/Mat1510>

ISSN:1665-2738, issn-e: 2395-8472

1 Introduction

The current public awareness about environmental issues like soil and water contamination, solid waste management, and energy savings for sustainable development is motivating the manufacture of greener materials (Tanasă *et al.*, 2019). It is in this sense that engineers and scientists working on fiber-reinforced polymer composites are turning their attention back to the development and use of renewable and biodegradable bio-based fibers (Martín del Campo *et al.*, 2020). Lignocellulosic fibers are among the most widely explored fibers as they provide high strength at low weight loadings, and because they are probably the most abundant fibers in nature. Moreover, the lignocellulosic fibers are much less abrasive than the synthetic ones, making the composite processing easier and cost-effective (Mutjé *et al.*, 2006). Also, the production of reinforcing bio-based fibers can involve less energetic and pollutant processes than those employed for the manufacture of the synthetic ones (Alhuthali *et al.*, 2013); however, vegetal fibers possess some unfavorable properties such as flammability, moisture absorption, and relatively low thermal stability (Takhur and Singha, 2015). It is, therefore, necessary to make some chemical treatments to render them suitable for multiple applications (Del Rey *et al.*, 2017; Brunengo *et al.*, 2019). A variety of surface treatments allow the extraction of lignin, hemicellulose, oils, waxes, and other low molar mass components (de Melo *et al.*, 2017; Pickering *et al.*, 2016). Such treatments enhance compatibility, reinforcing capacity, and thermal stability of lignocellulosic fibers, usually by mercerization and chemical modification of their surface. For instance, Gurunathan *et al.* (2015) reported that alkaline solutions had been used to bleach and mercerize lignocellulosic fibers, improving their thermal stability and reinforcement capacity in composites. These bleached fibers can exhibit tensile strength and modulus as high as 1110 MPa and 70 GPa, respectively. Recently, cold plasma treatment, a solvent-free and non-pollutant option, has been used to improve the surface properties of fibers to make them suitable for polymer reinforcement. For instance, Baltazar-y-Jimenez *et al.* (2008) studied the effect of an atmospheric-pressure air plasma jet on the thermal stability of “unbleached” hemp fibers. They found an increase of 30 °C in the thermal resistance of hemp fibers after 1 min of air plasma treatment. Other fibers, such as luffa (Abdel-Fattah *et al.*, 2019) and

flax yarn (Seghini *et al.*, 2019), exhibited a significant improvement in thermal stability when treated with cold plasma. Improving the thermal stability of natural fibers must allow their incorporation into high melting temperature polymers with minor detrimental effects on their structural integrity and properties. As far as we know, there are few or no literature reports on bleached hemp fibers modified with air plasma under reduced or atmospheric pressure. Herein, we discuss the effect of low and atmospheric pressure air cold plasma treatments on the morphology and thermal stability of bleached hemp fibers. The main purpose of the present study is to demonstrate the capability of air plasma treatments to increase the thermal stability of bleached hemp fibers, making them less susceptible to degradation during composite processing.

2 Materials and methods

2.1 Fibers preparation and plasma treatments

Commercial bleached hemp (CBH) fibers, with average diameter and length of 22 μm and 1.34 mm, respectively (Alonso-Montemayor *et al.*, 2020), were provided by CELESA S. A. (Tortosa, Spain). Fibers were dispersed in distilled water, obtaining a thick pulp, which was compressed into 6.25 cm^2 square wafers (1 mm average thick) that were dried for 24 h in an oven set at 70 °C. The dried wafers were treated on both sides in a low-pressure rotatory plasma (LPRP) at 13.56 MHz, 2.1×10^{-1} mbar, and 100 W, as well as with an atmospheric-pressure plasma jet (APPJ) at 65 kHz, 1013 mbar, and 100 W. LPRP consisted of a low-pressure reaction chamber equipped with a 500 mL round bottom flask, rotating at 50 rpm to ensure a homogeneous modification and a copper coil that induced the electromagnetic field. Wafers were treated with air LPRP for 30 and 180 min (samples labeled LPP 30 and LPP 180, respectively). In LPRP treatments, residual air was used as process gas. On the other hand, APPJ is a high voltage plasma jet device operated at 6 kV and 17 mA (~ 100 W). The gap between the plasma needle and the wafer surface was 1 cm, and the airflow was 12.4 L min^{-1} . A 6.25 cm^2 square wafer of CBH fibers was treated for 15 s (labeled as Jet sample) under atmospheric conditions. By using a sample holder, this square wafer was displaced under the jet plume to expose its surface to plasma. Figure 1 shows the LPRP and APPJ devices.

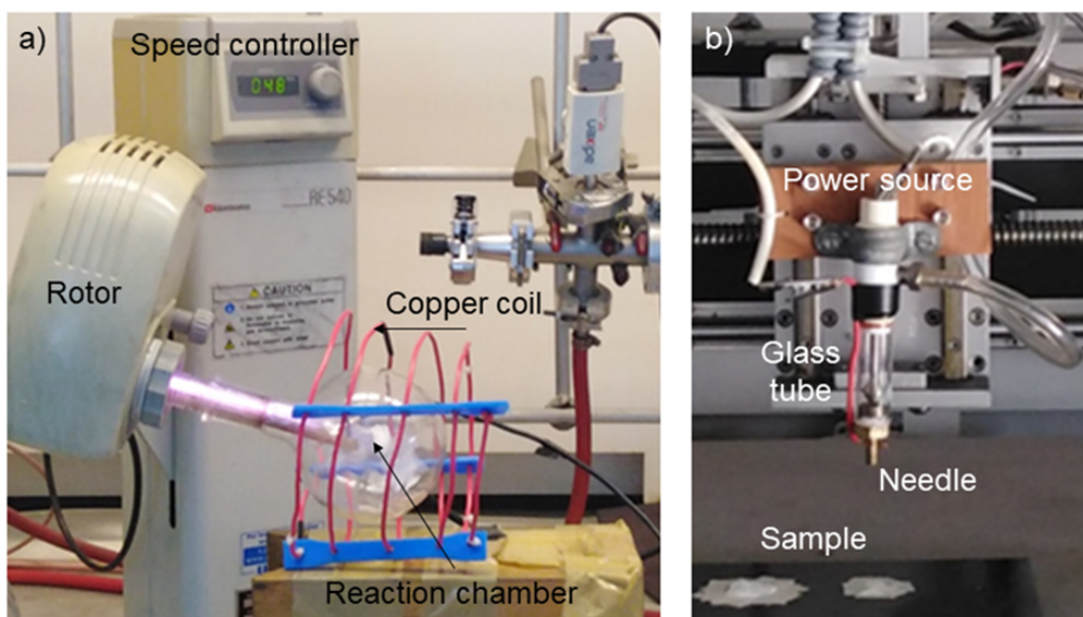


Fig. 1.) LPRP and b) APPJ home-made devices.

2.2 Instrumental analyses

The chemical composition of fibers was evaluated by Fourier transform infrared spectroscopy–attenuated reflectance mode (FTIR-ATR) employing a Perkin Elmer Frontier FTIR spectrometer. FTIR-ATR spectra were recorded in a 600-4000 cm^{-1} range, 16 scans, and 4 cm^{-1} resolution. The FTIR spectra were normalized for comparison.

The crystalline characteristics of fibers were determined with a Panalytical Empyrean X-ray diffractometer (XRD) with Cu $K\alpha$ radiation ($\lambda=0.154$ nm) at 40 kV and 30 mA. The XRD patterns were recorded in the scattering angle range of $2\theta=10$ to 50° with a step size of 0.02° . The upper surface of samples was carefully leveled with the sample holder boards by using a flat glass plate. The distance between cellulose chains at the 002 plane (d_{002}) was calculated by using Eq. (1) (Bragg's law), where λ is the wavelength (0.154 nm) of the incident X-rays and θ_{002} is the Bragg angle. The apparent crystallite size (L) and the proportion of crystallite interior chains (X) were calculated through Eqs. (2) and (3), respectively, where K is the Scherrer constant (0.94), H_{002} is the half-height width of the 002 diffraction peak in radians, and h is the layer thickness of the surface chain (0.57 nm) (Poletto *et al.*, 2013; Toba *et al.*, 2013). Finally, Seagal's crystallinity index (Crl) was also determined by means of Eq. (4), where Crl is the relative degree of crystallinity, I_{002} is the maximum

intensity of the 002 peak (at $2\theta \approx 23^\circ$) and I_{am} is the intensity at $2\theta \approx 18.5^\circ$ (Abdullah *et al.*, 2019; Liu *et al.*, 2019; Padovani *et al.*, 2019). Crl was developed by Segal *et al.* (1959) for cellulosic materials. In this study, all diffraction patterns were normalized for I_{002} .

$$d_{002} = \frac{\lambda}{2 \sin \theta_{002}} \quad (1)$$

$$L = \frac{K\lambda}{H_{002} \cos \theta_{002}} \quad (2)$$

$$X = \frac{(L - 2h)^2}{L^2} \quad (3)$$

$$Crl = \frac{I_{002} - I_{am}}{I_{002}} \times 100 \quad (4)$$

The morphological characteristics of the CBH fibers were examined in a Top Con 510 SM scanning electron microscope (SEM) operated at 10 kV. CBH fibers were coated with a thin Au–Pd layer before analysis.

The thermal stability was evaluated by thermogravimetric analysis (TGA) performed with a Pekin Elmer TGA 4000 under inert atmosphere (N_2), at a heating speed of $20^\circ\text{C min}^{-1}$ from 30 to 600°C . Changes in thermal stability higher than 5°C were attributed to plasma-treatment and not to experimental error. TGA was performed by using a representative sample of each air plasma treated fiber.

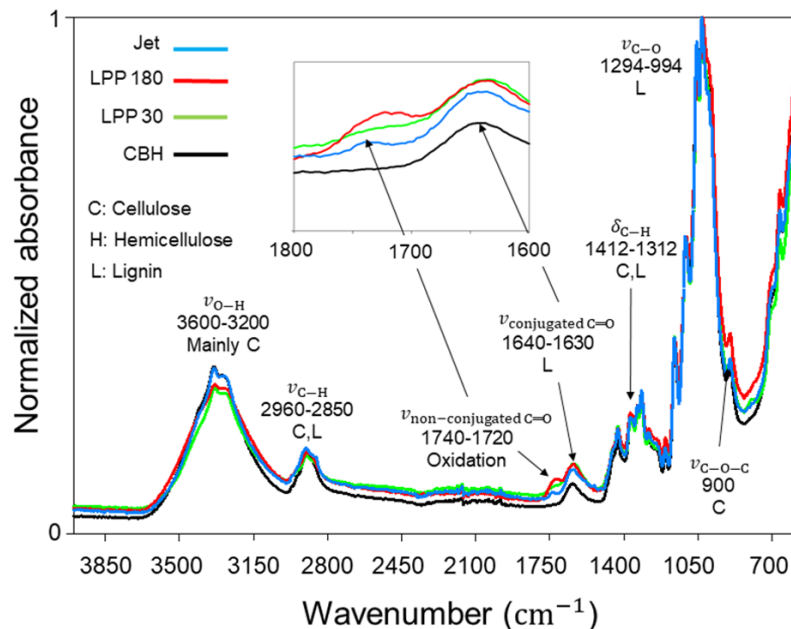


Fig. 2. Infrared spectra of the untreated and air plasma-treated CBH. The stretching band between 1720 and 1740 cm^{-1} is attributed to the C = O groups of the oxidized cellulose by air plasma species. This band is absent only in the untreated CBH.

3 Results and discussion

3.1 Chemical composition

In raw lignocellulosic fibers, cellulose microfibrils are bonded together by an amorphous interphase. The surface layers of fibers are rich in lignin and hemicellulose, while the internal structure is mainly composed of microfibril bundles of cellulose. In bleached lignocellulosic fibers, lignin and hemicellulose are removed from the surface, and cellulose becomes the main component. As known, cellulose is a linear polysaccharide containing glucose molecules joined by β -glycoside linkages (Takhur and Singha, 2015). Figure 2 shows the FTIR spectra of untreated and plasma-treated bleached hemp fibers. As it can be noted, most bands correspond to cellulose; bands associated with lignin and hemicellulose are barely appreciated. The FTIR bands were attributed as follows: A broad stretching band of the O–H bonds ($\nu_{\text{O-H}}$) between 3600 to 3200 cm^{-1} ; a low-intense stretching band of the CH_2 and CH_3 groups ($\nu_{\text{C-H}}$) around 2960 to 2850 cm^{-1} . These later groups also show a bending band ($\delta_{\text{C-H}}$) from 1412 to 1312 cm^{-1} ; a C–O stretching band ($\nu_{\text{C-O}}$) from 1294 to 994 cm^{-1} (Moonart and Utara, 2019). Also, a

typical $\nu_{\text{C-O-C}}$ band appearing at 900 cm^{-1} , and that is related to β -glycoside linkages of cellulose. The slight increase of this band was attributed to crosslinking between the cellulose chains. It is to point out here that crosslinking is one of the expected reactions in plasma treatments. (Macedo *et al.*, 2020a; Alonso-Montemayor *et al.*, 2017). The low intense $\nu_{\text{conjugated C=O}}$ band, characteristic of lignin, appears between 1630 and 1640 cm^{-1} (Kalia and Kumar, 2013; Araujo *et al.*, 2013; Lu and Oza, 2013; Oza *et al.*, 2011; Bar *et al.*, 2019). Other bands of lignin may appear at 1507 and 1458 cm^{-1} for C = C bonds and aromatic skeletal vibration, respectively (Macedo *et al.*, 2020b). These bands are overlapped with the $\delta_{\text{C-H}}$ bands. On the other hand, the lack of a band at 1730 cm^{-1} in the infrared spectrum of the untreated CBH suggests the absence of hemicellulose. This band is typically attributed to $\nu_{\text{non-conjugated C=O}}$ of hemicellulose of raw fibers (Moonart and Utara, 2019). In plasma-treated fibers, a low intense band appeared between 1720 and 1740 cm^{-1} , but it was attributed to the plasma induced-oxidation of fibers rather than to the presence of hemicellulose (indicating the absence of this compound on the fiber surface). The rise of this band was associated with the presence of carbonyl groups which were inserted in the cellulose chains by means of the air plasma treatments.

In studying flax yarns treated with O₂ plasma, Seghini *et al.* (2019) observed a similar stretching band at 1741 cm⁻¹ that they attributed to the formation of carbonyl and carboxyl species. Air plasma contains O₂-based reactive species like O^{2•} and HO[•] (N₂ is less reactive than O₂) according to the following reactions: O₂ + e⁻ → 2O^{2•} + e⁻ and H₂O + γ^{UV} or e⁻ → 2HO[•] + 2H^{UV}. Particularly, e⁻, whose kinetic energy is around 20 to 28 eV (Fridman, 2008; de Souza *et al.*, 2020), can easily break C–O, C–H, and O–H bonds, which are present in cellulose and their bond energy is only 3.6, 4.3, and 4.8 eV, respectively (Ebewele, 2000).

3.2 Crystallinity

The X-ray diffraction patterns of both untreated and treated CBH fibers are depicted in Figure 3. The diffraction peaks appearing from 14 to 16°, 16 to

18°, 22 to 24°, and 33 to 36° are one-to-one related to the 101, 10 $\bar{1}$, 002, and 040 planes of cellulose I (Abdullah *et al.*, 2019). It is worth mentioning that cellulose I is found in two crystalline forms: monoclinic (I β) and triclinic (I α) structures, coexisting in various proportions. The X-ray patterns correspond to the coexistence of both crystalline forms, although I β is the dominant polymorph (Poletto *et al.*, 2011; Poletto *et al.*, 2013). It can be noticed that the plasma treatment caused a slight displacement of the diffraction peaks towards lower angles. This displacement is interpreted as an increase in the interplanar distances (see Table 1), and it happens when polymer chains are functionalized with small chemical groups, separating them from one another (Moonart and Utara, 2019). The increment of the interplanar distances is in line with the formation of the new carbonyl groups (band at 1640 cm⁻¹) detected by FTIR analysis. It should be highlighted that, the effect plasma treatment on the interplanar distance between cellulose chains of bleached fibers is reported here for the first time.

Table 1. Crystallographic properties of the untreated and treated CBH.

Sample	I_{am}	θ_{002} (rad)	H_{002} (rad)	d_{002} (nm)	L (nm)	X	Crl (%)
CBH	0.125	0.201	0.0258	0.378	5.7	0.64	88
LPP 30	0.122	0.199	0.0269	0.383	5.5	0.63	88
LPP 180	0.112	0.199	0.0264	0.383	5.6	0.64	89
Jet	0.115	0.198	0.0267	0.385	5.5	0.63	89

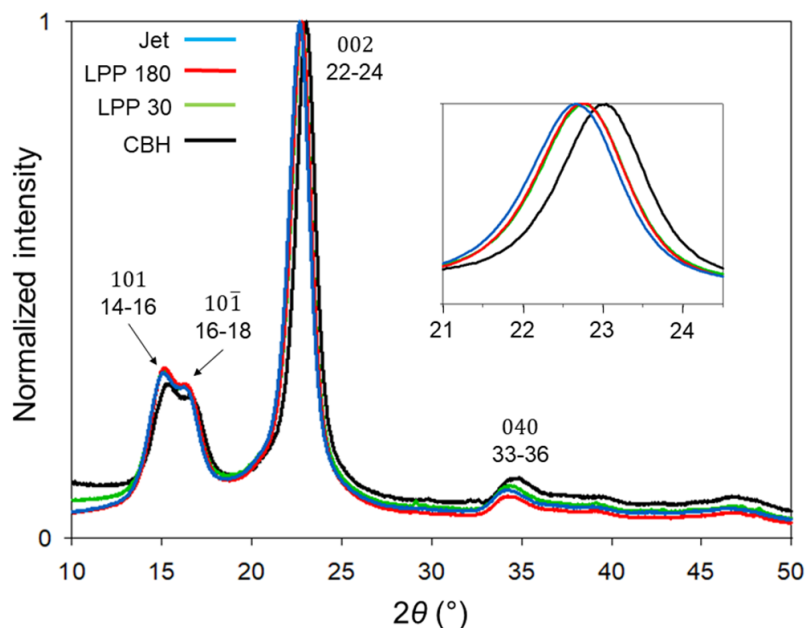


Fig. 3. X-ray diffraction patterns of both untreated and air plasma-treated CBH.

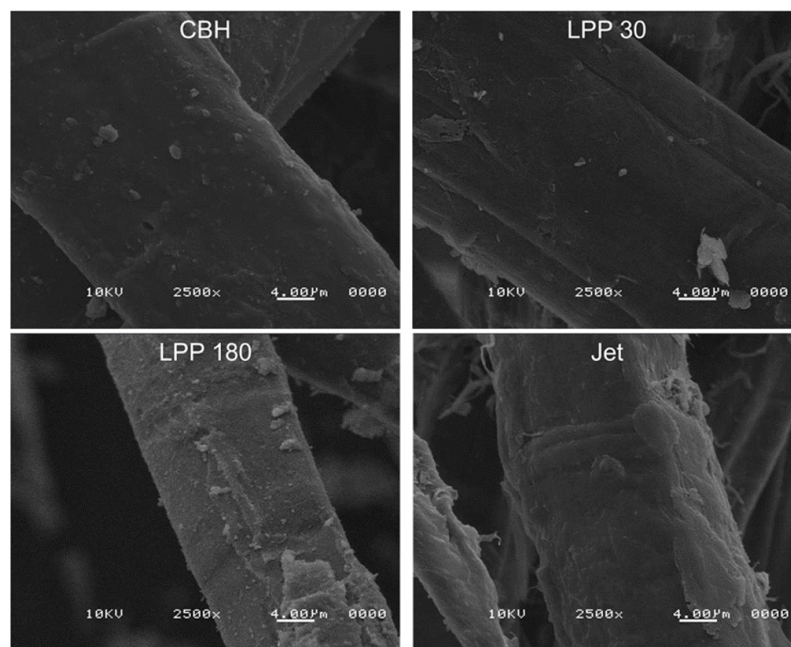


Fig. 4. SEM images of the untreated and air plasma-treated CBH fibers.

3.3 Morphology

Figure 4 shows SEM images of the untreated and plasma-treated CBH fibers. It can be seen that the surface of the untreated fiber (CBH sample) is smooth with minor defects. On the contrary, the surface of plasma treated fibers is rough, especially that of the LPP 180 sample, which looks as if the outer layers were removed causing thinning and severe surface damages. The plasma jet treated fiber (Jet sample) also showed lots of irregularities, but its surface remained rather smooth. For plasma-treated lignocellulosic fibers, it is expected that chemical interactions between oxygen ions and the outmost surface layers of fibers produce oxidation and crosslinking, both reflected in surface defects like low roughness and low etching damages (Baltazar-y-Jimenez *et al.*, 2007; de Farias *et al.*, 2017). Such defects were indeed produced in LPP 30 and Jet samples and could be useful for the mechanical interlocking with polymers. For LPP 180 sample, the prolonged exposition time to high energetic plasma species also produced oxidation and crosslinking, but it is clear that it caused severe etching and other eroding defects. Similar results have been reported for APPJ (using Ar as process gas) treated bleached hemp fibers, which exhibited surface stratification after plasma treatment (Brunengo *et al.*, 2019). In this regard, the SEM results can support the FTIR findings since the presence of erosion may

involve the grafting of functional groups into the fiber surface (Abdel-Fattah *et al.*, 2019). It is necessary to consider that erosion occurs by a chemical etching process during plasma treatment. The reaction of the air plasma species with the fiber surface can produce changes in the surface morphology (Seghini *et al.*, 2019).

3.4 Thermal stability

As already mentioned, the thermal stability of fibers might be improved to avoid degradation when they are used in processes involving high temperatures (> 200 °C) like the preparation of fiber-reinforced polymers through melt processing. Plasma treatment allows improving the thermal stability of lignocellulosic fibers through cross-linking and grafting of carbonyl groups. The increase in carbonyl groups grafted into cellulose chains, as FTIR analysis indicates, must lead to an improvement of the thermal stability of CBH by the formation of hydrogen bonds within neighboring cellulose chains (Poletto *et al.*, 2013). Figure 5 displays the TGA traces of the untreated and plasma-treated CBH. From 30 to 100 °C, a loss weight of 2 to 4 wt%, associated with moisture, is observed. As expected for bleached fibers, samples did not exhibit any loss weight from 130 and 230 °C related to extractive components (sugars, fats, chlorophyll, among others), lignin, and hemicellulose

degradations (Santos *et al.*, 2007; Almeida *et al.*, 2019; Rodríguez-Soto *et al.*, 2019). The pronounced weight loss (up to 80 wt%) around 300 °C is mainly associated with cellulose degradation (Khan *et al.*, 2006). It can be noticed that the treated fibers are, in general, more thermally stable than the untreated one. For instance, despite the short exposure time, the Jet sample exhibited an initial degradation temperature (T_g) of around 290 °C. This temperature is 30 °C higher than that of the untreated CBH; such an increment was attributed to the use of high voltage

plasma. Baltazar-y-Jimenez *et al.* (2008) found a similar increase in thermal resistance for jet treated raw hemp fibers; although, it should be pointed out that they did their experiments with unbleached hemp fibers. LPP 30 and LPP 180 fibers showed T_{deg} of around 275 °C and 260 °C, respectively, suggesting for the later an over exposition (Baltazar-Y-Jimenez *et al.*, 2009). Plasma treatment of bleached fibers is, therefore, an excellent strategy to improve the thermal stability, although the plasma exposition time might be carefully adjusted for optimal results.

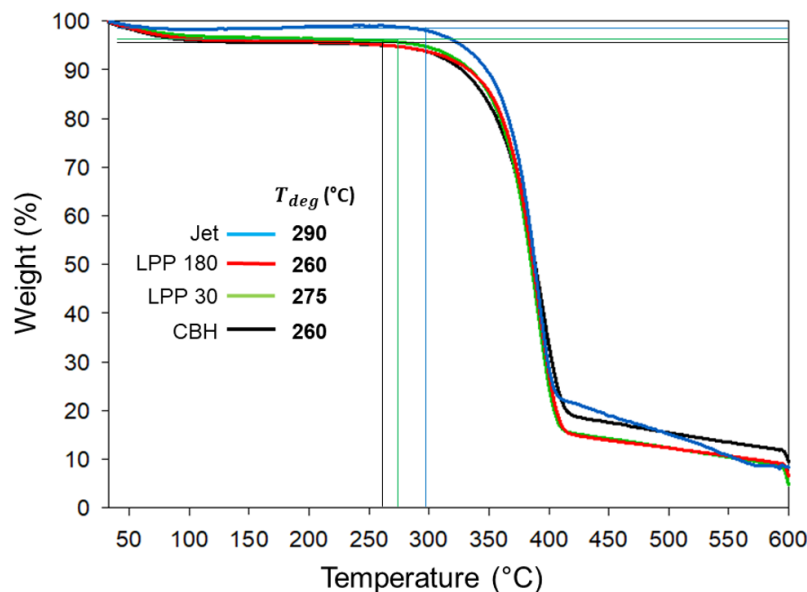


Fig. 5. Thermogravimetric curves of the untreated and air plasma-treated CBH fibers.

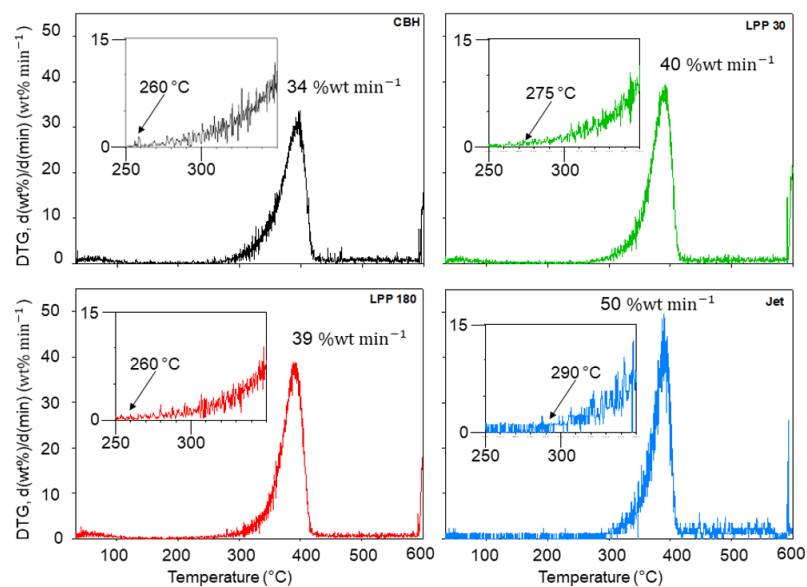


Fig. 6. First derivative of the TGA (DTG) curves of the untreated and air plasma-treated CBH fibers.

The thermal decomposition behavior of the untreated and air plasma treated CBH fibers was also evaluated by means of the first derivatives of TGA (DTG). Figure 6 shows the DTG of the untreated and air plasma-treated CBH fibers. Insertions show that the onset degradation temperatures, calculated from DTG, correspond well to those calculated from TGA thermographs. Moreover, it was found that all fibers (treated and untreated) reached their maximal weight loss ratio around 400 °C; although the LPP 30 and Jet fibers exhibited a retardation effect characterized by a high weight loss at the highest decomposition speed. The maximal weight loss ratio of these two fibers is around 40 and 50 wt% min⁻¹, respectively, whereas for the LPP 180 and CBH fibers, is only of 39 and 34 wt% min⁻¹, respectively. It has been reported that plasma treatment accentuates the weight loss ratio of exposed lignocellulosic fibers (Abdel-Fattah, 2019). Thus, when highly thermally resistant fibers reach their temperature of maximal degradation speed, they can lose more material than the less thermally resistant fibers. Also, it must be noted that the CBH fiber does not exhibit a broad peak (around 300 °C) attributed to the thermal decomposition of hemicellulose (Macedo *et al.*, 2020b). Thus, both DTG and FTIR analyses indicate that there is no detectable amount of hemicellulose in the CBH fibers.

Conclusions

The surface treatment of commercial bleached hemp (CBH) fiber with low-pressure rotatory plasma (LPRP) and atmospheric-pressure plasma jet (APPJ) produced chemical and morphological changes that enhanced its thermal stability. By FTIR analysis, it was found that both air plasma treatments allowed the introduction of carbonyl groups and promoted the formation of glycoside linkages. These two chemical changes were associated with the functionalization and cross-linking of cellulose, which is the main component of the outmost layers of bleached hemp fibers. By XRD analysis, it was encountered that the interplanar distance (d_{002}) between cellulose chains, increased with plasma treatment. This increment was attributed to the insertion of carbonyl groups. Through SEM analysis, it was found that treated fibers became rougher than the untreated one, especially the CBH fiber treated by LPRP during 180 min, and for which the surface damage was severe. Through TGA it was found that LPRP (30 min treatment) and APPJ

treatments increased the thermal resistance of the CBH fiber in 15 °C and 30 °C, respectively. Longer experiments with LPRP (180 min) caused a significant eroding without improving the thermal resistance. Results here presented indicate that the cold plasma surface modification of bleached hemp fibers may assist with mechanical interlocking when used in polymer reinforcing, with good thermal resistance during processing.

Acknowledgements

FJAM thanks the Consejo Nacional de Ciencia y Tecnología (CONACYT) of Mexico for the grant (627977) given to pursuit his MSc degree in Materials Science and Technology at UAdeC. FJAM also thanks CONACYT for supporting a three months research stay at the University of Girona (UdG), Spain.

Nomenclature

H_{002}	Half-height width of the 002 plane diffraction peak
I_{002}	Intensity of the 002 plane diffraction peak
I_{am}	Minimum intensity at $2\theta \approx 18.5^\circ$
T_{deg}	Initial degradation temperature
d_{002}	Distance between cellulose chains calculated from the 002 plane diffraction peak
θ_{002}	Bragg angle of the 002 plane diffraction peak
APPJ	Atmospheric-pressure plasma jet equipment
CBH	Commercially bleached hemp fibers
FTIR-ATR	Fourier transform infrared spectroscopy—attenuated reflectance mode
h	Layer thickness of the surface cellulose chains (0.57 nm)
Jet sample	Atmospheric-pressure plasma jet treated CBH
LPP 180	sample Low-pressure plasma-treated CBH for 180 min
LPP 30	sample Low-pressure plasma-treated CBH for 30 min
LPRP	Low-pressure rotatory plasma device
RF	Radiofrequency
SEM	Scanning electron microscopy
TGA	Thermogravimetric analysis
XRD	X-ray diffraction
Crl	Seagal's crystallinity index

K Scherrer constant (0.94)
 L Apparent crystallite size
 X Proportion of crystallite interior chains
 λ Wavelength

References

- Abdel-Fattah, E. (2019). Surface and thermal characteristics relationship of atmospheric pressure plasma treated natural luffa fibers. *The European Physical Journal D* 73, 1-8.
- Abdullah, C., Azzahari, A., Rahman, N., Hassan, A., Yahya, R. (2019). Optimizing treatment of oil palm-empty fruit bunch (OP-EFB) fiber: Chemical, thermal and physical properties of alkali treated fibers. *Fibers and Polymers* 20, 527-537.
- Acayanka, E., Tarkwa, J., Laminsi, S. (2019). Evaluation of energy in a batch and circulating non-thermal plasma reactors during organic pollutant oxidation in aqueous solution. *Plasma Chemistry and Plasma Processing* 39, 75-87.
- Alhuthali, A., Low, M. (2013). Mechanical properties of cellulose fibre reinforced vinyl-ester composites in wet conditions. *Journal of Materials Science* 48, 6331-6340.
- Almeida, F., Meili, L., Soletti, J., Esquerre, K., Ribeiro, L., de Farias Silva, C. (2019). Oil produced water treatment using sugarcane solid residue as biosorbent. *Revista Mexicana de Ingeniería Química* 18, 27-38.
- Alonso-Montemayor, F., Narro-Céspedes, R., Oliva-Castañeda, A. (2017). Surface modification by plasma applications on lignocellulosic fibers. *Journal of BioProcess and Chemical Technology* 9, 21-26.
- Alonso-Montemayor, F., Tarrés, Q., Oliver-Ortega, H., Espinach, F., Narro-Céspedes, R., Castañeda-Facio, A., Delgado-Aguilar, M. (2020). Enhancing the mechanical performance of bleached hemp fibers reinforced polyamide 6 composites: A competitive alternative to commodity composites. *Polymers* 12, 1041.
- Araujo, J., Adamo, C., Costa e Silva, M., De Paoli, M. (2013). Antistatic-reinforced biocomposites of polyamide-6 and polyaniline-coated curauá fibers prepared on a pilot plant scale. *Polymer Composites* 34, 1081-1090.
- Baltazar-Y-Jimenez, A., Bismarck, A. (2007). Surface modification of lignocellulosic fibres in atmospheric air pressure plasma. *Green Chemistry* 9, 1057-1066.
- Baltazar-Y-Jimenez, A., Bistriz, M., Schulz, E., Bismarck, A. (2009). Atmospheric air pressure plasma treatment of lignocellulosic fibres: impact on mechanical properties and adhesion to cellulose acetate butyrate. *Composites Science and Technology* 68, 215-227.
- Baltazar-y-Jimenez, A., Juntaro, J., Bismarck, A. (2008). Effect of atmospheric air pressure plasma treatment on the thermal behaviour of natural fibers and dynamical mechanical properties of randomly-oriented short fiber composites. *Journal of Biobased Materials and Bioenergy* 2, 264-272.
- Bar, M., Das, A., Alagirusamy, R. (2019). Influence of flax/polypropylene distribution in twistless thermally bonded rovings on their composite properties. *Polymer Composites* 40, 1-12.
- Brisset, J., Pawlat, J. (2016). Chemical effects of air plasma species on aqueous solutes in direct and delayed exposure modes: Discharge, post-discharge and plasma activated water. *Plasma Chemistry and Plasma Processing* 36, 355-381.
- Brunengo, E., Conzatti, L., Utzeri, R., Vicini, S., Scatto, M., Falzacappa, E., Castellano, M., Stagnaro P. (2019). Chemical modification of hemp fibres by plasma treatment for eco-composites based on biodegradable polyester. *Journal of Materials Science* 54, 14367-14377.
- de Farias, J., Cavalcante, R., Canabarro, B., Viana, H., Scholz, S., Simão, R. (2017). Surface lignin removal on coir fibers by plasma treatment for improved adhesion in thermoplastic starch composites. *Carbohydrate Polymers* 165, 429-436.
- de Melo, R., Marques, M., Navard, P., Duque, N. (2017). Degradation studies and mechanical properties of treated curauá fibers and microcrystalline cellulose in composites with polyamide 6. *Journal of Composite Materials* 51, 1-9.

- Del Rey, R., Serrat, R., Alba, J., Perez, H., Mutje, P., Espinach, F. (2017). Effect of sodium hydroxide treatments on the tensile strength and the interphase quality of hemp core fiber-reinforced polypropylene composites. *Polymers* 9, 377-391.
- de Souza, I.A., de Medeiros Neto, J.F., Nascimento, I.O., Matamoros, E.P., Feitor, M.C., Fernandes, F.M., Magalhães Sousa, R.R., de Carvalho Costa, T. H. (2020). Triple langmuir probe, optical emission spectroscopy and lissajous figures for diagnosis of plasma produced by dielectric barrier discharge of parallel plates in atmospheric pressure. *International Journal of Applied Electromagnetics and Mechanics (Preprint)*, 1-11.
- Ebewele, R. (2000). *Polymer Science and Technology*. CRC press LLC, Florida.
- Fridman, A. (2008). *Plasma chemistry*. Cambridge University Press, New York.
- Gurunathan, T., Mohanty, S., Nayak, S.K. (2015). A review of the recent developments in biocomposites based on natural fibres and their application perspectives. *Composites Part A* 77, 1-25.
- Kalia, S., Kumar, A. (2013). Surface modification of sunn hemp fibers using acrylation, peroxide and permanganate treatments: a study of morphology, thermal stability and crystallinity. *Polymer-Plastics Technology and Engineering* 52, 24-29.
- Khan, F., Ahmad, S., Kronfli, E. (2006). γ -Radiation induced changes in the physical and chemical properties of lignocellulose. *Biomacromolecules* 7, 2303-2309.
- Liu, Y., Xie, J., Wu, N., Ma, Y., Menon, C., Tong, J. (2019). Characterization of natural cellulose fiber from corn stalk waste subjected to different surface treatments. *Cellulose* 26, 4707-4719.
- Lu, N., Oza, S. (2013). Effect of surface treatment of hemp fibers on the thermal stability of the hemp-PLA (poly lactic acid) composites. *Advanced Materials Research* 651, 499-504.
- Macedo, M., Silva, G., Feitor, M., Costa, T., Ito, E., Melo, J. (2020a). Composites from recycled polyethylene and plasma treated kapok fibers. *Cellulose* 27, 2115-2134.
- Macedo, M., Silva, G., Feitor, M., Costa, T., Ito, E., Melo, J. (2020b). Surface modification of kapok fibers by cold plasma surface treatment. *Journal of Materials Research and Technology* 9, 2467-2476.
- Martín del Campo, A., Robledo-Ortiz, J., Arellano, M., Jasso-Gastinel, C., Silva-Jara, J., López-Naranjo, E., Pérez-Fonseca, A. (2020). Glycidyl methacrylate as compatibilizer of poly(lactic acid)/nanoclay/agave fiber hybrid biocomposites: Effect on the physical and mechanical properties. *Revista Mexicana de Ingeniería Química* 19, 455-469.
- Moonart, U., Utara, S. (2019). Effect of surface treatments and filler loading on the properties of hemp fiber/natural rubber composites. *Cellulose* 26, 7271-7295.
- Mutjé, P., Vallejos, M., Gironès, J., Vilaseca, F., López, A., López, P., Méndez, J. (2006). Effect of maleated polypropylene as coupling agent for polypropylene composites reinforced with hemp strands. *Journal of Applied Polymer Science* 102, 833-840.
- Oza, S., Wang, R., Lu, N. (2011). Thermal and mechanical properties of recycled high density polyethylene/hemp fiber composites. *International Journal of Applied Science and Technology* 1, 31-36.
- Padovani, J., Legland, D., Pernes, M., Gallos, A., Thomachot-Schneider, C., Shah, D., Bourmand, A., Beaugrand, J. (2019). Beating of hemp bast fibres: an examination of a hydromechanical treatment on chemical, structural, and nanomechanical property evolutions. *Cellulose* 26, 5665-5683.
- Pickering, K., Aruan Efendy, M., Le, T. (2016). A review of recent developments in natural fibre composites and their mechanical performance. *Composites Part A* 83, 98-112.
- Poletto, M., Vinícios, P., Zeni, M., Zattera, A. (2011). Crystalline properties and decomposition kinetics of cellulose fibers in wood pulp obtained by two pulping processes. *Polymer Degradation and Stability* 96, 679-685.
- Poletto, M., Zattera, A., Pistor, V. (2013). Structural characteristics and thermal properties of native cellulose. In: *Cellulose - Fundamental Aspects*

- (T. van de Ven y Godbout, L., eds.), Pp. 45-70. InTech, Rijeka.
- Rodríguez-Soto, K., Piñeros-Castro, N., Ortega-Toro, R. (2019). Laminated composites reinforced with chemically modified sheets-stalk of *Musa cavendish*. *Revista Mexicana de Ingeniería Química* 18, 749-758.
- Santos, P., Spinacé, M., Feroselli, K., De Paoli, M. (2007). Polyamide-6/vegetal fiber composite prepared by extrusion and injection molding. *Composites Part A* 38, 2404-2411.
- Segal, L., Creely, J., Martin, A., Conrad, C. (1959). An empirical method for estimating the degree of crystallinity of native cellulose using the X-ray diffractometer. *Textile Research Journal* 29, 786-794.
- Seghini, M., Touchard, F., Sarasini, F., Chocinski-Arnault, L., Tirillò, J., Bracciale, M., Zvonek, M., Cech, V. (2019). Effects of oxygen and tetravinylsilane plasma treatments on mechanical and interfacial properties of flax yarns in thermoset matrix composites. *Cellulose* 27, 511-530.
- Takur, V., Singha, A. (2015). *Surface Modification of Biopolymers*. John Wiley & Sons, New Jersey.
- Tanasă, F., Zănoagă, M., Teacă, C., Nechifor, M., Shahzad, A. (2019). Modified hemp fibers intended for fiber-reinforced polymer composites used in structural applications—A review. I. Methods of modification. *Polymer Composites* 41, 5-31.
- Thirumdas, R., Sarangapani, C., Annapure, U. (2015). Cold plasma: A novel non-thermal technology for food processing. *Food Biophysics* 10, 1-11.
- Toba, K., Yamamoto, H., Yoshida, M. (2013). On the mechanical interaction between cellulose microfibrils and matrix substances in wood cell walls: effects of chemical pretreatment and subsequent repeated dry-and-wet treatment. *Journal of Wood Science* 59, 359-366.
- Torres-Segundo, C., Vergara-Sánchez J., Reyes-Romero, P., Gómez-Díaz, A., Rodríguez-Albarrán, M., Martínez-Valencia H. (2019). Effect on discoloration by nonthermal plasma in dissolved textile dyes: Acid black 194. *Revista Mexicana de Ingeniería Química* 18, 939-947.